The Dimethylamine Dimer Ion Is an Ion−Radical Complex: A Combined TPEPICO, Variational RRKM, and *ab Initio* MO Study of the Fragmentation of Ionized Dimers of Dimethylamine

Paul M. Mayer,[†] Jeffrey W. Keister, and Tomas Baer*

Chemistry Department, University of North Carolina, Chapel Hill, North Carolina 27599-3290

Matt Evans and C. Y. Ng

Ames Laboratory, U.S. Department of Energy, and Department of Chemistry, Iowa State University, Ames, Iowa 50011

Chia-Wei Hsu

Chemical Sciences Division, Lawrence Berkeley National Laboratory, Berkeley, California 94720

Received: August 30, 1996; In Final Form: December 9, 1996[⊗]

Threshold photoelectron photoion coincidence spectroscopy has been used to study the fragmentation mechanism of dimethylamine dimer ions. The fragmentation rate constant data obtained from the experiment were modeled with variational RRKM theory using potential energies and vibrational frequencies from *ab initio* molecular orbital calculations at the MP2/6-31G* level. The results are consistent with the fragmentation of the dimethylamine dimer ion into protonated dimethylamine and the $^{\bullet}CH_2N(H)CH_3$ radical. This was supported by *ab initio* calculations in which the dimer ion was found to consist of a N−H−C hydrogen-bonded complex between the above two products. The RRKM fit to the experimental $k(E)$ vs E data for the ion gave a dimethylamine dimer ion $\Delta_f H^\circ_0$ of 653 ± 11 kJ mol^{-1} and thus a dimer ion binding energy of 147 ± 16 kJ mol^{-1}. In agreement with recent experimental results, the neutral dimethylamine dimer was calculated to be an N−H−N hydrogen-bonded dimer with a 0 K binding energy of 13 ± 3 kJ mol^{-1}. The resulting neutral dimer adiabatic ionization energy is 6.8 ± 0.2 eV.

Introduction

Clusters of organic molecules can be viewed as intermediate between the dilute gas phase and the condensed phase. When ionized, they tend to dissociate via one of two pathways:

$$M_n^{\bullet+} \rightarrow M_{n-1}^{\bullet+} + M \qquad \text{type 1}$$

$$M_n^{\bullet+} \rightarrow M_{n-1}R^+ + (M-R)^{\bullet} \qquad \text{type 2}$$

where $M_n^{\bullet+}$ is an ionized cluster of n monomers and R is a radical, typically hydrogen. Type 1 clusters tend to be bound by van der Waals forces (e.g., Ar_n, $(C_6H_6)_n$) while type 2 tend to be H-bonded clusters (e.g., $(CH_3OH)_n$ and $((CH_3)_2NH)_n$).

A great deal of experimental and computational effort has been expended in order to understand the structure, bonding, reactivity, and thermochemistry of neutral and ionized clusters. Most of the experimental data on ionic clusters has come from high-pressure mass spectrometry[1] and multiphoton ionization/time-of-flight (TOF) mass spectrometry[2] which have provided information about the equilibria between different sized cluster ions. In high-pressure mass spectrometry cluster ions are formed by ion−molecule reactions between an ionized and neutral molecule. For type 2 clusters, this usually forms the ions above their fragmentation thresholds and thus only the $M_{n-1}R^+$ fragment ions are observed in the mass spectrum. Multiphoton ionization of neutral clusters formed in a molecular beam also may form type 2 cluster ions above their dissociation limits because of the often poor Franck−Condon overlap between the neutral and ion potential energy surfaces. In these cases, the above techniques provide relative enthalpies of the $M_{n-1}R^+$ fragmentation products.

Threshold photoelectron photoion coincidence (TPEPICO) spectroscopy[3] is one of the most versatile experimental techniques available for studying the fragmentation mechanisms and thermochemistry of ions. Work from this lab has shown that it can be used successfully to study type 1 cluster ions[4] and that intact molecular ions of hydrogen-bonded dimers can be observed in the coincidence TOF mass spectra.[5]

Most neutral clusters are formed only at low temperatures. Thus TPEPICO studies, which ionize such neutral clusters, must employ a supersonic molecular beam source. When ions are extracted perpendicular to the direction of the molecular beam, the TOF distribution of the parent ion is extremely narrow because of the low translational temperature (~4 K) orthogonal to the beam axis. While the TOF peaks of the molecular ions, $M^{\bullet+}$ or $M_n^{\bullet+}$, are narrow, the ion peaks which are produced by dissociative photoionization typically are broader by a factor of 10. This is a direct result of kinetic energy release (KER).[5] Thus, ions formed by the direct ionization of a neutral molecule or cluster can easily be distinguished from those formed in dissociative processes. This is a distinct advantage over high-pressure mass spectrometry or other techniques which generate cluster ions by gas-phase ion−molecule reactions in which the precursor to a particular cluster ion is often unknown.

In this paper we report a study of the thermochemistry and fragmentation mechanism of dimethylamine dimer ions with TPEPICO spectroscopy. The neutral hydrogen-bonded dimer,

* Corresponding author.
[†] Present address: Research School of Chemistry, Australian National University, Canberra, ACT 0200, Australia.
[⊗] Abstract published in *Advance ACS Abstracts,* January 15, 1997.

S1089-5639(96)02707-7 CCC: $14.00

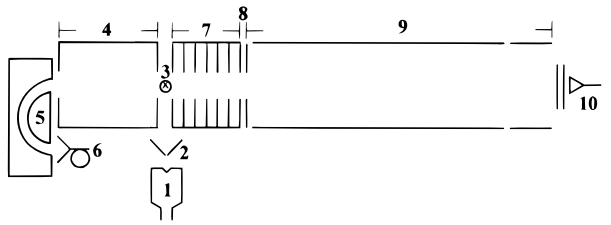

Figure 1. Schematic diagram for the UNC and ALS TPEPICO instruments. (1) Molecular beam nozzle with orifice (UNC, 70 mm; ALS, 127 mm); (2) skimmer (ALS instrument has two skimmers); (3) photoionization region; (4) steradiancy analyzer (UNC, 7.2 cm, +12.3 V; ALS, 12.8 cm, +6 V); (5) hemispherical analyzer; (6) electron detector, (UNC, channeltron; ALS, microchannel plate); (7) first acceleration region (UNC, 5 cm, 20 V/cm; ALS, 7.4 cm, 10 V/cm); (8) second acceleration region (UNC, 0.25 cm, 397 V/cm; ALS, 0.6 cm, 134 V/cm); (9) field-free drift tube (UNC, 31 cm; ALS, 44 cm); (10) ion detector (UNC, microchannel plate; ALS, El-Mol microsphere plate).

when ionized, fragments to form the protonated dimethylamine ion and a radical which can either be $^{\bullet}CH_2N(H)CH_3$ or $(CH_3)_2N^{\bullet}$ (i.e., they are type 2 dimers). The rate constant for the fragmentation has been measured as a function of dimer ion internal energy and the data modeled with microcanonical variational transition state theory (VTST).[6,7] *Ab initio* calculations were used to investigate the bonding and structure of the neutral and ionic dimer as well as transition state structures for the RRKM/VTST analysis.

The Experiment

The experiments discussed in this paper were carried out on two instruments, one at the University of North Carolina (UNC) and the other on the Chemical Dynamics Beamline at the Advanced Light Source (ALS) of the Lawrence Berkeley National Laboratories. The major difference in the two experiments is the light source and photon resolution. The other features of the two TPEPICO apparatus are essentially the same, the differences being some of the distances and voltages applied to the various regions of the two instruments. A schematic diagram is shown in Figure 1. The UNC instrument has been described in detail elsewhere.[4] Sample molecules were ionized in the ion source (3) with vacuum ultraviolet (VUV) light from an H_2 discharge lamp energy selected by a 1 m monochromator (having a photon energy resolution of 15 meV). Threshold electrons were selected by the steradiancy (4) and hemispherical analyzers (5) (~15 meV electron energy resolution) and detected with an electron multiplier (6). The resulting ion was detected in coincidence with the electron, the time difference between the two detection events defining the ion time-of-flight (TOF). A multichannel analyzer software package (MAESTRO version 3.01, EG&G Ortec, Oakridge, TN) was used to collect the coincidence events. The spectra were obtained with a TOF resolution of 10.5 ns but were rebinned to 42 ns resolution to obtain better statistics for the rate constant fitting process.

Photoionization of sample molecules in the ion source of the ALS instrument was carried out with radiation from a 10 cm undulator in the synchrotron beam line.[8] Higher order harmonics from the undulator were suppressed by an argon gas filter.[9] The energy of the VUV radiation was selected by a 6.65 m McPherson monochromator (1200 grooves/mm grating) with a photon energy resolution of 1.3 meV. The storage ring was operated in multibunch mode thereby producing a quasi-continuous VUV radiation source (478 MHZ pulse rate). Threshold electrons were selected by a steradiancy analyzer consisting of a 12.8 cm drift tube held at a potential of +6 V relative to the ion source. The electrons are detected after passing through the hemispherical analyzer, providing the start pulse for a Stanford Research Systems SR430 multichannel scaler. The energy resolution of the detected threshold electrons was ~15 meV. The ions were detected by an El-Mul Microsphere Plate detector providing the stop pulse for the SR430. The TOF bin size was 5 ns, but the data were rebinned to 50 ns resolution to obtain better statistics for the rate constant fitting procedure.

The sample was introduced into the ion source of both instruments in the form of a continuous molecular beam. At UNC, 100 Torr of dimethylamine was introduced into 200 Torr of argon to give 300 Torr of backing pressure to a 70 mm nozzle orifice. At the ALS, 300 Torr of dimethylamine was seeded into 1200 Torr of argon to provide 2 atm backing pressure to a 127 mm nozzle orifice. Similar TOF mass spectra were observed in both experiments. Typical counting times were 24−48 h on the UNC instrument and 3 h at ALS.

Ab Initio and Microcanonical Variational Transition State Theory (μVTST) Calculations

Ab initio molecular orbital calculations were carried out on a Convex C3840 Supercomputer at the University of North Carolina using the Gaussian 92[10] package and a Cray T-916 at the North Carolina Supercomputing Facility using the Gaussian 94[11] package. Geometries at potential energy minima were optimized at the MP2/6-31G* level. The neutral dimer binding energy was obtained at both the MP2/6-31G*//MP2/6-31G* and the MP2/6-311+G**//MP2/6-31G* levels of theory. The energy of the dimer relative to the sum of two optimized monomers was corrected for basis set superposition error (BSSE) using the counterpoise (CP) technique.[12] It has been demonstrated that the counterpoise technique is useful in determining binding energies of hydrogen-bonded dimers as it tends to give consistent results over a large range of basis sets.[13]

The dissociation of the dimer ion was modeled with the following μVTST (or variational RRKM theory) expression:[6,7,14,15]

$$k(E) = \frac{\sigma}{h}\frac{N^{\ddagger}(E,E_0,R^*)}{\rho(E)} \qquad (1)$$

where $k(E)$ is the unimolecular rate constant at an ion internal energy, E, σ is the reaction symmetry number, h is Planck's constant, E_0 is the activation energy, $\rho(E)$ is the reactant ion density of states, and $N^{\ddagger}(E,E_0,R^*)$ is the sum of states for the fragmentation bottleneck located at an intracluster separation R^*. The value of R^* is obtained by finding the minimum reaction flux along the reaction coordinate. The density and sum of states calculations employed the "steepest-descent" approach of Forst.[15,16]

Results and Discussion

The Data. A typical coincidence mass spectrum of supersonically cooled dimethylamine, DMA, obtained with the UNC apparatus is shown in Figure 2a. Present in the spectrum are peaks due to cluster fragment ions $(DMA)_nH^+$ ($n = 1-4$) and the intact dimer ion $(DMA)_2^{\bullet+}$ (Figure 2b). The dimer ion peak is the only one with a narrow TOF distribution. This shows that it is the only ion produced directly from its neutral precursor. All other ions are produced by dissociative ionization which results in broadened peaks because of kinetic energy release in the dissociation. Eight more spectra were obtained over a

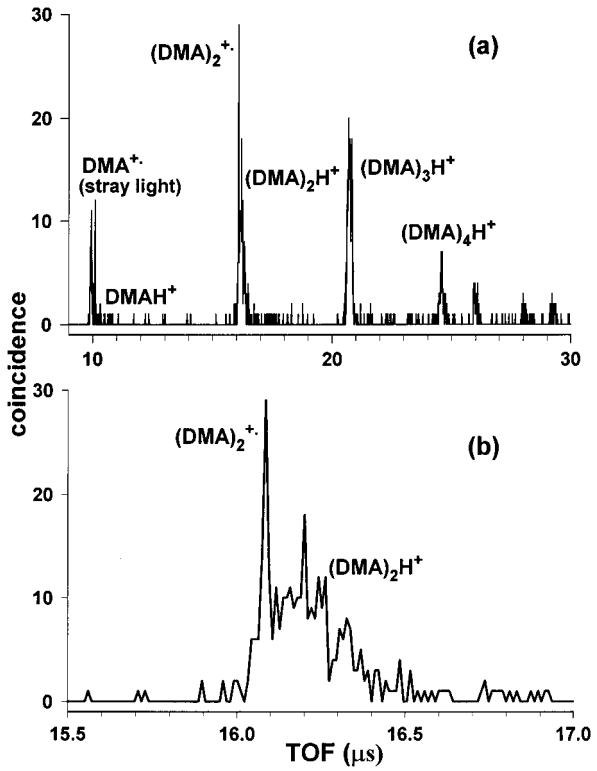

Figure 2. TOF mass spectrum of dimethylamine clusters at a photon energy of 8.09 eV: (a) protonated dimethylamine clusters ions which are formed by dissociative ionization of higher order clusters; (b) expanded view of (a) showing the presence of intact dimethylamine dimer ions. This spectrum, obtained on the UNC apparatus, was acquired for 27 h.

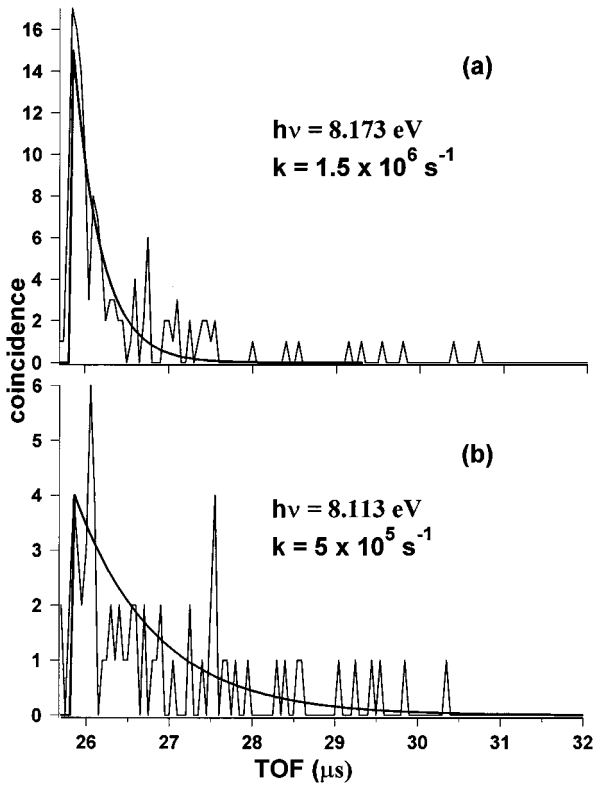

Figure 3. Examples of the modeling of the $DMAH^+$ peak with unique rate constants for two photon energies: (a) 8.17 eV and (b) 8.11 eV. These spectra were obtained on the ALS apparatus. The TOF differ from those in Figure 2 because of the smaller extraction field and different acceleration regions.

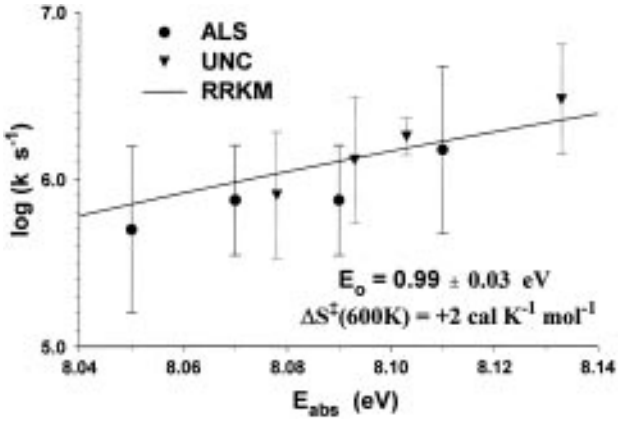

Figure 4. Plot of the experimental log($k(E)$) vs absolute energy data (● = ALS, ▼ = UNC) and the RRKM $k(E)$ curve for the simple bond cleavage of the dimer ion to form $^{\bullet}CH_2N(H)CH_3$ as obtained by the variational transition state theory procedure outlined in the text.

photon energy range of 8.09−8.19 eV. When dimethylamine was introduced at 298 K, no cluster ions were observed.

Dimer ions which fragment in the first acceleration region of the instruments (section 7 in Figure 1) produce $DMAH^+$ fragment ion peaks with an asymmetric TOF distribution that can be modeled with a single-exponential decay rate constant. The signal-to-noise ratio for the TOF data is low due to the low counting rates. The rates were low on the UNC apparatus because of low light intensity. At the Chemical Dynamics Beamline of the ALS, the counting rates are low because of low collection efficiency for electrons and ions. This apparatus is not yet optimized for PEPICO experiments. As a result, there is significant error inherent in the fitting procedure. Calculated peak TOF profiles were obtained for unimolecular rate constants of 1, 2.5, 5, and 7.5×10^5 s^{-1} and 1, 1.5, and 2.5×10^6 s^{-1}, and the results compared with the experimental TOF distributions to determine the most reasonable value for k at each photon energy. Two examples of the modeling of data obtained at the ALS are shown in Figure 3. The results for the UNC and ALS data are shown in Figure 4 plotted as log($k(E)$) vs absolute energy, E_{abs}. The absolute energy for the rate data was obtained by adding the photon energy for each point to the neutral dimethylamine dimer heat of formation, $\Delta_f H°_0 = -6 \pm 3$ kJ mol^{-1}, obtained from *ab initio* calculations (see the following section). The average internal thermal energy of the neutral dimers was taken to be zero. The error introduced by this assumption is less than the 13 ± 3 kJ mol^{-1} binding energy of the dimer.

The $DMAH^+$ ion could be due to the fragmentation of not only the dimer ion but higher order clusters as well. Two arguments against this hypothesis can be made. First, we note from the breakdown diagram (not shown here) that the $DMAH^+$ product ion builds up precisely as the sharp $(DMA)_2^+$ peak decreases thereby identifying the latter species as the parent ion. Second, the rate constant for the $DMAH^+$ formation from the trimer ion will be significantly lower than that from the dimer ion because the trimer will be lower in energy and have a greater density of states (more vibrational modes). Thus, the formation of $DMAH^+$ from higher order clusters can be ignored in the present study. Similarly, we ignore any possible trimers of the form $(DMA)_2Ar^+$ because no such trimers were observed in the mass spectrum. Their concentration is expected to be much smaller than those of the more stable $(DMA)_n$ clusters.

There are two possible radical products for the fragmentation of the dimethylamine dimer ions which correspond to the intracluster transfer of either a methyl hydrogen or the amine hydrogen:

TABLE 1: Tabulated Heats of Formation (kJ mol^{-1})

	$\Delta_f H°_0$	$\Delta_f H°_{298}$	ref[a]
$(CH_3)_2NH$	$+3.5 \pm 0.4$	-18.5 ± 0.4	17
$(CH_3)_2NH^{\bullet+}$	796 ± 8	776 ± 8	17
$(CH_3)_2NH_2^+$	605	580	*b*
$^{\bullet}CH_2N(H)CH_3$	144 ± 8	126 ± 8	17
$(CH_3)_2N^{\bullet}$	162 ± 8	145 ± 8	17
$[(CH_3)_2NH]_2$	-6 ± 3	-48 ± 3	*ab initio*—present work
	-8	-50	20
$[(CH_3)_2NH]_2^{\bullet+}$	653 ± 11	611 ± 11	RRKM—present work
	686	644	*ab initio*—present work
	750	708	21

[a] 298 K values from ref 17 corrected to 0 K using frequencies in Table 3. [b] From the proton affinity (PA) of dimethylamine, PA_{298K} = 932 kJ mol^{-1}, PA_{0K} = 926 kJ mol^{-1}.[18,19]

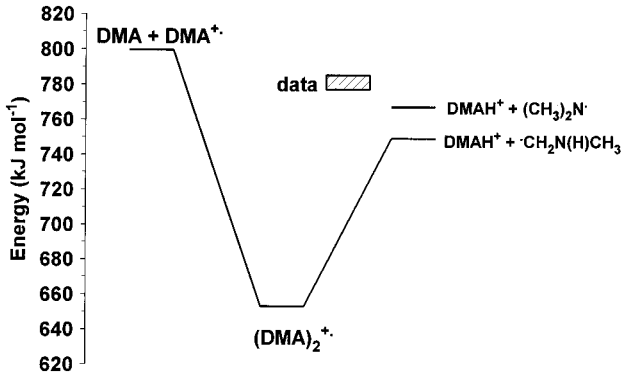

Figure 5. Potential energy surface for the unimolecular fragmentation of dimethylamine dimer ions. The energy range of the experimental data in Figure 4 is shown in the box.

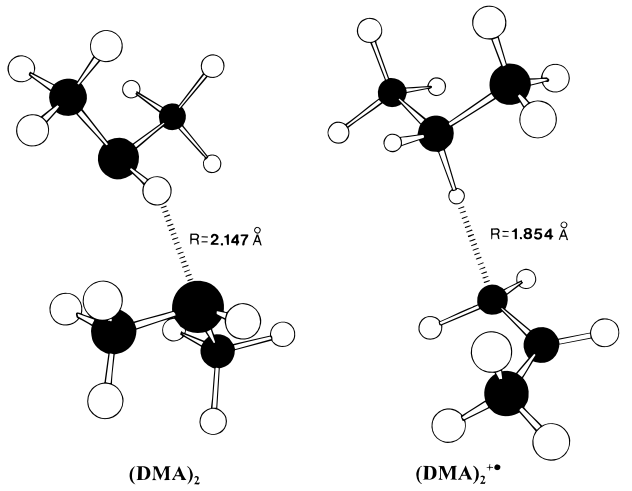

Figure 6. Calculated geometries of the neutral and ionic dimers of dimethylamine at MP2/6-31G*.

$$(DMA)_2^{\bullet+} \rightarrow DMAH^+ + {}^{\bullet}CH_2N(H)CH_3$$

$$(DMA)_2^{\bullet+} \rightarrow DMAH^+ + (CH_3)_2N^{\bullet}$$

Table 1 lists the $\Delta_f H°$ values for the species on the potential energy surface shown in Figure 5. The experimental $k(E)$ data lie higher in energy than either pair of fragmentation products so that, on energetic grounds, either could be formed.

***Ab Initio* Calculations.** The structure of the neutral dimer is shown in Figure 6 along with the intermolecular bond distance. The neutral contains an N−H hydrogen bond of 2.147 Å. No other stable orientation of the two monomers could be found on the MP2/6-31G* surface. The relative energy of the dimer compared to two monomers at both the MP2/6-31G* and MP2/6-311+G** levels are shown in Table 2. There is a significant correction to the binding energy by BSSE which is typical of hydrogen-bonded dimer energies calculated at the MP2 level.[13] The calculated 0 K neutral dimer binding energy was chosen to be 13 ± 3 kJ mol^{-1}, the MP2/6-311+G** value. The error limits were chosen to include both the MP2/6-31G* value and the literature experimental value (Table 1). The quoted precision is sufficient for our purposes in the present study. The above binding energy gives $\Delta_f H°_0$ ((DMA)$_2$) = -6 ± 3 kJ mol^{-1} and thus $\Delta_f H°_{298}$ ((DMA)$_2$) = -48 ± 3 kJ mol^{-1}. The 298K value is obtained from the 0 K value by the use of the calculated vibrational frequencies, Table 3. The present value is similar to an experimental determination of the binding energy by Lambert and Strong,[20] 15 kJ mol^{-1} (0 K). They measured the deviation of the second virial coefficient for dimethylamine vapor from that predicted by the Berthelot equation to obtain the dimerization equilibrium constant at several temperatures. A van't Hoff plot then gave the heat of dimerization.

TABLE 2: Calculated Neutral Dimer Binding Energies (BE)

	$(CH_3)_2NH + (CH_3)_2NH$	$[(CH_3)_2NH]_2$
E(MP2/6-31G*)[a]	−269.330 596 6	−269.340 594 9
E(MP2/6-311+G**)[a]	−269.556 763 4	−269.565 535 6
ZPE[b]	471.4	475.5
BE(MP2/6-31G*)		10 (22)[c] kJ mol^{-1}
BE(MP2/6-311+G**)		13 (19)[c] kJ mol^{-1}
		15[d] kJ mol^{-1}

[a] Units of hartrees. [b] From the vibrational frequencies in Table 3, in kJ mol^{-1}. [c] The value without BSSE correction is in parentheses. [d] Reference 20.

The structure in Figure 6a is consistent with that deduced to be the lowest energy conformer from microwave spectroscopy by Tubergen and Kuczkowski[23] (their structure 2B), including the nonlinear hydrogen bond. From Stark shift measurements, they deduced the components of the dipole moment to be 1.50, 0.0, and 0.84 D. These agree very well with our calculated dipole moments of 1.55, 0.0, and 0.90 D. However, on the basis of a distributed multipole analysis of the dimer structure using MP2 correlation and Dunning's DZP basis set, Wales *et al.*[24] found a second conformer, 1 kJ/mol lower in energy. This structure has a nonlinear hydrogen bond, but the two monomers are in a near-parallel arrangement. When this arrangement was optimized at the MP2/6-31G* level of theory in the present study, it in fact rearranged to the structure in Figure 6a. Because of the small value of the energy difference between these two conformers and the low barrier between them, the results may be very sensitive to the level of the basis set and electron correlation. Finally, the dipole moments calculated by Wales *et al.* for the two isomers (2.06, 0.58, 0.95; 1.61, 0.29, 1.56) do not match very well with the experimental values. On the other hand, the binding energies of the Wales *et al.* dimers of 15 and 14 kJ/mol agree with our value of 13 ± 3 kJ/mol.

When the neutral dimer in Figure 6a was optimized as a radical cation, the geometry minimized to a dimer ion consisting of a protonated dimethylamine monomer hydrogen bonded to the methylene group of a $^{\bullet}CH_2N(H)CH_3$ radical, Figure 6. The charge and spin densities also support this assignment. We found no structure for the dimer ion that resembled in any way the structure of the neutral dimer. In view of the dimer ion structure, it is highly likely that the radicals formed in the fragmentation of dimethylamine dimer ions are $^{\bullet}CH_2N(H)CH_3$. The formation of the higher energy neutral radical would require a rearrangement. The 0 K binding energy of the ion (relative to DMA + DMA$^{\bullet+}$) was calculated to be 114 kJ mol^{-1}, yielding $\Delta_f H°_0$((DMA)$_2^{\bullet+}$) = 686 kJ mol^{-1} and hence $\Delta_f H°_{298}$((DMA)$_2^{\bullet+}$)

TABLE 3: Calculated Vibrational Frequencies for Dimethylamine, Its Ion, Dimers, and Reaction Products

	harmonic frequencies (cm^{-1})[a]
$(CH_3)_2NH$	233, 272, 377, 788, 922, 999, 1068, 1146, 1160, 1235, 1407, 1437, 1437, 1458, 1472, 1485, 1491, 2855, 2857, 2967, 2968, 3016, 3017, 3343
$(CH_3)_2NH^{\bullet+}$	17, 76, 398, 551, 843, 977, 1019, 1035, 1113, 1203, 1377, 1379, 1391, 1422, 1428, 1452, 1470, 2887, 2893, 3011, 3072, 3073, 3344
$[(CH_3)_2NH]_2$	28, 50, 77, 90, 111, 175, 230, 249, 276, 293, 382, 385, 805, 873, 916, 967, 1000, 1011, 1065, 1070, 1137, 1151, 1161, 1167, 1234, 1241, 1401, 1406, 1430, 1433, 1436, 1456, 1460, 1471, 1475, 1475, 1484, 1489, 1493, 1511, 2846, 2848, 2869, 2870, 2954, 2956, 2975, 2977, 3006, 3007, 3022, 3022, 3282, 3337
$[(CH_3)_2NH]_2^{\bullet+}$	6, 50, 76, 110, 120, 163, 184, 230, 287, 374, 381, 412, 601, 859, 880, 933, 958, 995, 1015, 1037, 1072, 1101, 1204, 1223, 1238, 1301, 1375, 1407, 1411, 1430, 1437, 1450, 1458, 1459, 1466, 1471, 1473, 1503, 1514, 1632, 2309, 2919, 2967, 2967, 2979, 3009, 3053, 3072, 3073, 3075, 3075, 3085, 3289, 3440
transition state	6,[b] 29, 44, 64, 95, 163, 189, 274, 298, 372, 396, 639, 825, 857, 859, 938, 979, 994, 1024, 1028, 1105, 1205, 1219, 1237, 1278, 1360, 1407, 1411, 1434, 1435, 1443, 1453, 1458, 1460, 1468, 1470, 1472, 1505, 1628, 2777 2908, 2970, 2970, 2983, 3017, 3040, 3078, 3079, 3081, 3081, 3110, 3299, 3419
$(CH_3)_2NH_2^+$	192, 261, 371, 791, 838, 979, 991, 1042, 1206, 1235, 1344, 1383, 1411, 1437, 1455, 1456, 1469, 1471, 1623, 2973, 2973, 3085, 3085, 3087, 3087, 3245, 3307
$^{\bullet}CH_2N(H)CH_3$	206, 335, 380, 677, 757, 942, 1010, 1109, 1214, 1256, 1411, 1433, 1463, 1470, 1494, 2898, 2986, 3023, 3026, 3135, 3397
$(CH_3)_2N^{\bullet}$	66, 142, 420, 896, 910, 987, 999, 1177, 1179, 1375, 1398, 1441, 1456, 1462, 1474, 2870, 2875, 2933, 2937, 3020, 3021

[a] MP2/6-31G* scaled by 0.9427.[22] [b] Treated as a free rotor in the RRKM calculations (see text).

TABLE 4: Relative Energies (RE) for the Dimethylamine Dimer Ion and Fragmentation Products

	E (hartrees)	ZPE (kJ mol^{-1})	RE[a] (kJ mol^{-1})	RE_{expt}[b] (kJ mol^{-1})
$(CH_3)_2NH + (CH_3)_2NH^{\bullet+}$	−269.039 373 8	466	0	0
$[(CH_3)_2NH]_2^{\bullet+}$	−269.086 776 9	476	−114	-147 ± 16 -50[c]
$[(CH_3)_2NH]_2^{\bullet+}$ (vertical from neutral)	−269.044 307 9	476	−3	-5 ± 14[d]
$(CH_3)_2NH_2^+ + {}^{\bullet}CH_2N(H)CH_3$	−269.055 611 3	475	−33	−51
$(CH_3)_2NH_2^+ + (CH_3)_2N^{\bullet}$	−269.055 995 3	472	−37	−33

[a] Calculated energies relative to DMA + $DMA^{\bullet+}$ (including ZPE) at 0 K. [b] See Table 1. [c] Reference 21. [d] Based on the 8.3 ± 0.15 eV vertical IP from the PES of ref 25.

= 644 kJ mol^{-1}, Table 4. The *ab initio* calculations incorrectly predict the $^{\bullet}CH_2N(H)CH_3$ radical to lie higher in energy than $(CH_3)_2N^{\bullet}$.

Although no adiabatic ionization energy for the dimethylamine has been measured, Pradeep *et al.*[25] on the basis of a photoelectron spectroscopic study reported a vertical ionization energy of the dimethylamine dimer of 8.3 eV. Because of the difficulty in subtracting the contribution of the dimethylamine monomer signal, error limits of ±0.15 eV must be applied. This measured value is very close to our calculated value of 8.32 eV. Because of the broad PES peak, it is unfortunately not possible to extract an adiabatic IE from this PES. However, in accord with our calculations, it is evident that there is a large change in the geometry between the neutral and ionic dimer structures.

Variational RRKM Analysis. The mechanism chosen to model the experimental data is a barrierless simple bond cleavage reaction from $(DMA)_2^{\bullet+}$ to form $DMAH^+ + {}^{\bullet}CH_2N(H)CH_3$. This reaction can proceed from the dimer ion via a simple bond break without an intermediate rearrangement step. On the other hand, formation of the higher energy $(CH_3)_2N^{\bullet}$ product would require rearrangement, and the rate constant would be considerably smaller than that for the simple bond cleavage. Thus it is not expected to compete effectively with the formation of $^{\bullet}CH_2N(H)CH_3$.

Microcanonical variational transition state theory was employed to model the simple bond cleavage reaction. The energy of the dimer ion, without optimization, was calculated for several intracluster separations ranging from the 1.854 Å equilibrium value to 11.854 Å, Figure 7. The curve comes to an asymptote at large separations where the energy was referenced to the experimental product heats of formation. The reaction path does not have a barrier and hence it is not possible to locate a unique transition state with *ab initio* MO calculations. It was necessary to locate the transition state by finding the intracluster separation, *R**, responsible for the minimum reaction flux. To do this, the vibrational frequencies at each point along the curve in Figure 7 were modeled in the following way. By comparing their calculated atomic displacements, the 54 normal modes of the dimer ion were assigned to $DMAH^+$ frequencies, $^{\bullet}CH_2N(H)CH_3$ frequencies, or one of the six modes which are converted

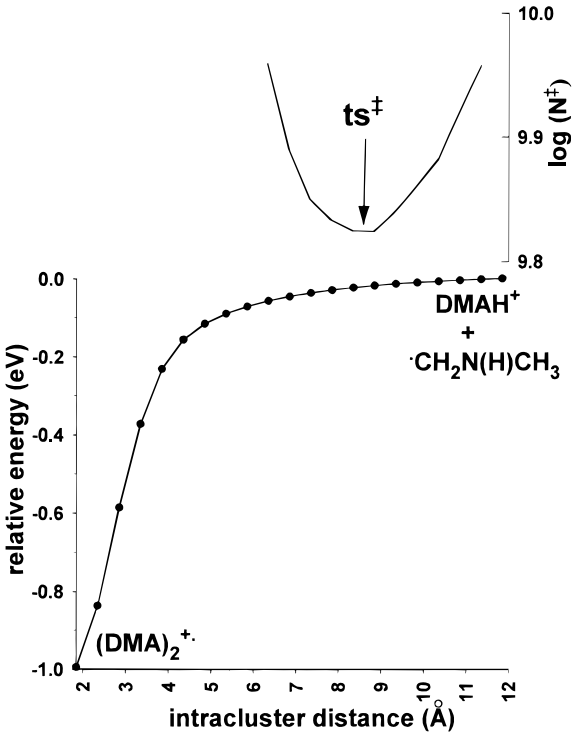

Figure 7. Calculated potential energy profile for the fragmentation of the dimethylamine dimer ion. The energy is relative to the experimental heats of formation of $DMAH^+ + {}^{\bullet}CH_2N(H)CH_3$. The upper curve is the logarithm of the sum of states for each point along the profile at an absolute energy of 8.09 eV (0.33 eV above the fragmentation products) with the effective RRKM transition state indicated by an arrow.

to translational and rotational degrees of freedom of the products (vanishing modes). This is straightforward since the six vanishing modes are the only ones in which all of the atoms in the dimer ion are displaced. The other modes involve the displacement of either only the $DMAH^+$ half of the dimer or only the radical half and change only slightly from the dimer ion to the free products. For these modes the transition state frequencies were chosen to be the average of the dimer and free product frequencies and hence were the same for every point along the curve in Figure 7. The six dimer ion modes identified as vanishing modes were 6, 50, 76, 110, 163, and 381 cm^{-1}. These six modes include four intracluster bends, one torsion, and one stretch. The 6 cm^{-1} frequency was assumed to be the torsion mode and was treated as a free rotor in the RRKM calculations. The moment of inertia of the torsion was obtained from the *ab initio* calculations to be 97 amu $Å^2$. The highest frequency mode, 381 cm^{-1}, was assumed to be the intracluster stretching frequency which represents the reaction coordinate for the cleavage of the dimer ion. The four remaining vanishing frequencies were then scaled according to the following equation[15,26,27]

$$\nu'(R) = \nu(R_{eq})\, e^{-a(R-R_{eq})} \qquad (2)$$

where $\nu'(R)$ is the value of the frequency at an intracluster separation R, R_{eq} is 1.854 Å, and a is an adjustable parameter. This equation is based on the assumption that the four modes will vanish exponentially to zero along the reaction coordinate.[26,27]

The parameter a is adjustable and was chosen by comparing the above four vanishing frequencies with those calculated for optimized dimer structures having intracluster separations of 3.854 Å (30, 74, 80, and 139 cm^{-1}) and 5.854 Å (16, 40, 77, and 139 cm^{-1}). A value for a of 0.08 $Å^{-1}$ in eq 2 predicts transition state frequencies at the two values of R very close to the *ab initio* values and yields a minimum root-mean-square deviation of 14 cm^{-1}. This value of a is very different from that found for bond scission reactions in neutral molecules (for CH_3-CH_3, $a = 0.82$ $Å^{-1}$)[28] or the value used for the dissociation of bromobenzene ions ($a = 1$ and 2 $Å^{-1}$)[14] but is similar to that found for ion−molecule reactions ($Li^+ + H_2O$, $a = 0.1$ $Å^{-1}$).[29]

The log of the sum of states, $\log(N^{\ddagger})$, as a function of R was calculated at several absolute energies. As expected, the bottleneck of the dissociation reaction was found to move to lower values of R as the energy increases. In this case, R^* moves from 8.854 to 8.354 Å over the energy range of the experimental data. The upper curve of Figure 7 shows $\log(N^{\ddagger})$ for an absolute energy of 8.092 eV, the energy midpoint for the experimental data. An average value of 8.604 Å was chosen for R^* to model the $k(E)$ vs E_{abs} data. Normally, the transition state would be varied in the variational RRKM treatment as a function of energy. However, since the data lie in a small energy range, fixing the transition state at 8.604 Å is not expected to introduce significant error. The vibrational frequencies used in the ensuing RRKM analysis for this transition state are listed in Table 3. The resulting transition state was characterized by a $\Delta S^{\ddagger}(600\ K)$ of +8 J mol^{-1} K^{-1}, a reasonable value for a simple bond cleavage reaction. The data in Figure 4 were then modeled with the above transition state by adjusting the ground state energy of $(DMA)_2^{\bullet+}$, i.e., the activation energy. The best fit is shown in Figure 4 and represents an E_0 of 0.99 ± 0.03 eV (96 ± 3 kJ mol^{-1}). This activation energy produces a dimer ion $\Delta_f H°_0$ of 653 ± 11 kJ mol^{-1}, Table 1, and a neutral dimer adiabatic ionization energy of 6.8 ± 0.2 eV.

Conclusion

Values for the 0 K binding energies of the neutral and ionic dimers of dimethylamine, 13 ± 3 and 147 ± 16 kJ mol^{-1}, respectively, have been obtained by TPEPICO spectroscopy and *ab initio* MO calculations. The calculated geometry of the neutral is an N−H−N hydrogen-bonded dimer, while the ion was found to consist of an N−H−C-bonded complex between protonated dimethylamine and the $^{\bullet}CH_2N(H)CH_3$ radical. The rate constant for the dimer ion fragmentation was measured and found to be consistent with a simple cleavage to form the above two products. The resulting 0 K heats of formation of the neutral and ion are −6 ± 3 and 653 ± 11 kJ mol^{-1}, respectively, giving a neutral dimer adiabatic IE of 6.8 ± 0.2 eV.

The heat of formation of the dimer ion can be found in Table 1 along with that obtained from *ab initio* MO calculations and the photoionization work of Bisling and co-workers.[21] As in our work, synchrotron radiation was used to photoionize neutral clusters formed in a molecular beam. However, ionization and fragmentation onsets were obtained from signal threshold determinations, which are often ill-defined, and not from an analysis of kinetic data for internal energy selected ions. The differences are dramatic, especially in the ionization energy of the dimer. Their value is 7.8 ± 0.2 eV whereas the present result is 6.8 ± 0.2 eV, obtained from the difference between the ion and neutral dimer heats of formation. The problem with the threshold measurement is that upon ionization the neutral dimer rearranges to the $DMAH^+-{}^{\bullet}CH_2N(H)CH_3$ structure shown in Figure 6. Any ionization onset measurement will tend to reflect the vertical IE and not the true adiabatic IE. The appearance energy of the $DMAH^+$ ion is shifted to an energy higher than that of either pair of products by a slow initial rate constant (kinetic shift effect[30]) and does not relate the energies of the lower energy products to that of the neutral dimer. Thus, the nature of the fragmentation products, a true E_0, and dimer ion heat of formation could only be obtained from an analysis of the kinetic data.

It is somewhat disquieting that the dimer ion binding energy of 147 kJ/mol relative to DMAH + $DMAH^+$ derived from the μVTST calculation disagrees with the *ab initio* MO calculated value of 114 kJ/mol (see Table 4). We can offer no explanation for this discrepancy of 33 kJ/mol. If this were the only error between experiment and calculations, we might be tempted to question our experimental results. However, we noted previously that our *ab initio* MO calculations of the energy difference between the $^{\bullet}CH_2N(H)CH_3$ and $(CH_3)_2N^{\bullet}$ radicals are in error by 22 kJ/mol (Table 4).

Acknowledgment. T.B. thanks the Department of Energy for continuing financial support. C.W.H., M.E., and C.Y.N. acknowledge support by the Director, Office of Energy Research, Office of Basic Energy Sciences, Chemical Sciences Division of the U.S. Department of Energy under Contract No. W-7405-Eng-82 for the Ames Laboratory and Contract No. DE-AC 03-76SF00098 for the Lawrence Berkeley National Laboratory. P.M.M. thanks the Natural Sciences and Engineering Research Council of Canada for a Postdoctoral Fellowship during the tenure of which this work was completed. T.B. and P.M.M. also thank the North Carolina Supercomputing Facility for the generous grant of computer time.

References and Notes

(1) Meot-Ner, M. *J. Am. Chem. Soc.* **1992**, *114*, 3312.
(2) Wei, S.; Tzeng, W. B.; Castleman, A. W. *J. Phys. Chem.* **1991**, *95*, 8306.
(3) Baer, T. *Adv. Chem. Phys.* **1986**, *64*, 111.
(4) Booze, J. A.; Baer, T. *J. Chem. Phys.* **1993**, *98*, 186.

(5) Booze, J. A.; Baer, T. *J. Chem. Phys.* **1992**, *96*, 5541.
(6) Truhlar, D. G.; Garrett, B. C. *Acc. Chem. Res.* **1980**, *13*, 440.
(7) Pechukas, P. *Annu. Rev. Phys. Chem.* **1981**, *32*, 159.
(8) Koike, M.; Heimann, P. A.; Kung, A. H.; Namioka, T.; DiGennaro, R.; Gee, B.; Yu, N. *Nucl. Instrum. Methods Phys. Res. A.* **1994**, *347*, 282.
(9) Suits, A. G.; Heimann, P.; Yang, X.; Evans, M.; Hsu, C.-W.; Lu, K.-t.; Lee, Y. T.; Kung, A. H. *Rev. Sci. Instrum.* **1995**, *66*, 4841.
(10) Frisch, M. J.; Trucks, G. W.; Head-Gordon, M.; Gill, P. M. W.; Wong, M. W.; Foresman, J. B.; Johnson, B. G.; Schlegel, H. B.; Robb, M. A.; Replogle, E. S.; Gomperts, R.; Andres, J. L.; Raghavachari, K.; Binkley, J. S.; Gonzalez, C.; Martin, R. L.; Fox, D. J.; Defrees, D. J.; Baker, J.; Stewart, J. J. P.; Pople, J. A. *GAUSSIAN 92, Revision A*; Carnegie-Mellon University: Pittsburgh, PA, 1992.
(11) Frisch, M. J.; Trucks, G. W.; Schlegel, H. B.; Gill, P. M. W.; Johnson, B. G.; Robb, M. A.; Cheeseman, J. R.; Keith, T.; Petersson, G. A.; Montgomery, J. A.; Raghavachari, K.; Al-Laham, M. A.; Zakrzewski, V. G.; Ortiz, J. V.; Foresman, J. B.; Cioslowski, J.; Stefanov, B. B.; Nanayakkara, A.; Challacombe, M.; Peng, C. Y.; Ayala, P. Y.; Chen, W.; Wong, M. W.; Andres, J. L.; Replogle, E. S.; Gomperts, R.; Martin, R. L.; Fox, D. J.; Binkley, J. S.; Defrees, D. L.; Baker, J.; Stewart, J. P.; Head-Gordon, M.; Gonzalez, C.; Pople, J. P. *Gaussian 94, Revision D.1*; Carnegie-Mellon University: Pittsburgh, PA, 1995.
(12) Boys, S. F.; Bernardi, F. *Mol. Phys.* **1970**, *19*, 553.
(13) Novoa, J. J.; Planas, M.; Rovira, M. C. *Chem. Phys. Lett.* **1996**, *251*, 33.
(14) Lifshitz, C.; Louage, F.; Aviyente, V.; Song, K. *J. Phys. Chem.* **1991**, *95*, 9298.
(15) Baer, T.; Hase, W. L. *Unimolecular Reaction Dynamics: Theory and Experiments*; Oxford: New York, 1996.
(16) Forst, W. *Theory of Unimolecular Reactions*; Academic Press: New York, 1973.
(17) Lias, S. G.; Bartmess, J. E.; Liebman, J. F.; Holmes, J. L.; Levin, R. D.; Mallard, W. G. *Gas Phase Ion and Neutral Thermochemistry. J. Phys. Chem. Ref. Data Vol. 17, Suppl. 1*; NSRDS, U.S. Government Printing Office: Washington, DC, 1988.
(18) Smith, B. J.; Radom, L. *J. Am. Chem. Soc.* **1993**, *115*, 4885.
(19) Szulejko, J. E.; McMahon, T. B. *J. Am. Chem. Soc.* **1993**, *115*, 7839.
(20) Lambert, J. D.; Strong, E. D. T. *Proc. R. Soc. London A.* **1950**, *200*, 566.
(21) Bisling, P. G. F.; Ruhl, E.; Brutschy, B.; Baumgartel, H. *J. Phys. Chem.* **1987**, *91*, 4310.
(22) Pople, J. A.; Scott, A. P.; Wong, M. W.; Radom, L. *Isr. J. Chem.* **1993**, *33*, 345.
(23) Tubergen, M. J.; Kuczkowski, R. L. *J. Chem. Phys.* **1994**, *100*, 3377.
(24) Wales, D. J.; Stone, A. J.; Popelier, P. L. A. *Chem. Phys. Lett.* **1995**, *240*, 89.
(25) Pradeep, T.; Hegde, M. S.; Rao, C. N. R. *J. Mol. Spectrosc.* **1991**, *150*, 289.
(26) Hase, W. L. *J. Chem. Phys.* **1972**, *57*, 730.
(27) Quack, M.; Troe, J. *Ber. Bunsen-Ges. Phys. Chem.* **1974**, *78*, 240.
(28) Hase, W. L. *J. Chem. Phys.* **1976**, *64*, 2442.
(29) Hase, W. L. *Chem. Phys. Lett.* **1987**, *139*, 389.
(30) Lifshitz, C. *Mass Spectrom. Rev.* **1982**, *1*, 309.